Journal of Clinical & Experimental Ophthalmology

Michelson et al. J Clinic Experiment Ophthalmol 2011, S:4
DOI: 10.4172/2155-9570.S4-001

Case Report Open Access

Cluster Analysis of Glaucoma Patients Using the Retinal Nerve Fiber Layer Thickness of the Optic Nerve and DTI Parameters of the Optic Radiation

Georg Michelson[1,4,5], Simone Wärntges[1,5]*, Tobias Engelhorn[2], Ahmed El Rafei[3,4], Joachim Hornegger[3,4], and Arnd Doerfler[2]

[1]*Department of Ophthalmology, Germany*
[2]*Department of Neuroradiology, Germany*
[3]*Department of Computer Science - Pattern Recognition Lab, Germany*
[4]*Erlangen Graduate School in Advanced Optical Technologies (SAOT), Germany*
[5]*Interdisciplinary Center of Ophthalmologic Preventive Medicine and Imaging (IZPI), University Erlangen-Nuremberg, Erlangen, Germany*

Abstract

Background: In glaucoma the optic radiation may be affected by ascending degeneration and/or ageing. This study classified groups of patients who are distinguishable related to their age, retinal nerve fiber layer thickness (RNFL), axonal integrity (measured by fractional anisotropy and mean diffusivity) and demyelination (measured by radial diffusivity) of the optic radiations. The goal was to separate glaucoma-induced damage of the optic radiations from impairment caused by the ageing effect.

Design: Prospective comparative observational study.

Participants: Fourty-five patients diagnosed with glaucoma of different entities and 17 patients with vital papilla (mean age 57.5 ± 13.8 years).

Methods: Multimodal MRI including diffusion tensor imaging (DTI) of the optic radiations and measurement of the RNFL thickness by Spectralis Optical Coherence Tomography. Hierarchical cluster analysis selected the optimal number of patient groups. Data were corrected for age. The t-test and a multiple linear regression model were applied.

Main Outcome Measures: Fractional anisotropy, and mean, axial, and radial diffusivity.

Results: Four clusters, two middle-aged and two older groups with different RNFL thickness each but same age, were classified. Multiple linear regression analysis showed a significant effect of the RNFL thickness on fractional anisotropy, mean diffusivity, and radial diffusivity of the optic radiations in the older patients having the stronger RNFL reduction ($p = 0.019$, 0.021, and 0.010, respectively). The slope of the radial diffusivity versus RNFL was different between the two older groups ($p = 0.025$).

Conclusions: In middle-aged glaucoma patients with reduced RNFL we found no change in the optic radiation. An ascending degeneration to the optic radiation was not verifiable. In contrast, in older glaucoma patients with reduced RNFL the axonal integrity/ demyelination of the optic radiation was impaired. The impairment was significantly associated with loss of RNFL and ageing.

Introduction

Glaucoma is the leading cause of irreversible blindness in industrialized countries. Open angle glaucoma (OAG) accounts for about 50% of glaucoma blindness [1]. The pathophysiological mechanisms are not completely elucidated. Both experimental [2,3] and human post-mortem studies [4] have shown that in addition to the damage of retinal ganglion cells also the post-retinal magno- and parvocellular layers of the lateral geniculate nucleus and the primary visual cortex were impaired in glaucoma. Some of the 4th neurons in the lateral geniculate nucleus have died and surviving neurons were atrophic. A concomitant damage of the 3rd (optic nerve and optic tract) and the 4th (optic radiations, OR) neuron of the visual pathway as a result of pathomechanisms underlying ischemia cannot be excluded. There are associations between typical cerebral lesions, which account for cerebral ischemia and microvascular risk factors (i.e. arterial hypertension) [5,6], cerebrovascular [7] and cardiovascular diseases [8]. Additionally, anatomy and physiology of retinal arterioles were found to be similar to cerebral arterioles.

The new non-invasive technique of the diffusion tensor imaging (DTI) is suitable to reconstruct the visual pathway [9]. It is based on the magnetic resonance imaging (MRI) and allows for quantification of limited diffusion of water molecules along fiber tracts such as the visual pathway. DTI parameters give information about the anisotropy and diffusivity of the Brownian motion of water molecules. They may be derived from the so-called diffusion tensor [10]. The diffusion tensor can be represented by an ellipsoid, which is characterized by three eigenvalues (λ_1, λ_2, and λ_3) and three eigenvectors in a local frame of each image voxel. Diffusivity is estimated by the average of the three eigenvalues and anisotropy means that the diffusion has directionality in parts of the brain [11,12]. The fractional anisotropy (FA) gives information about the magnitude portion of the diffusion tensor caused by anisotropy [13,14]. The mean diffusivity (MD) represents the

***Corresponding author:** Simone Waerntges, MD, University of Erlangen-Nuremberg, Department of Ophthalmology, Interdisciplinary Center of Ophthalmologic, Preventive Medicine and Imaging (IZPI), Schwabachanlage 6, D-91054 Erlangen, Germany, Tel: +49 (9131) 853-4272; Fax: +49 (9131) 853-4271; E-mail: Simone.Waerntges@uk-erlangen.de

Received September 09, 2011; **Accepted** November 05, 2011; **Published** November 15, 2011

Citation: Michelson G, Wärntges S, Engelhorn T, Rafei AE, Hornegger J, et al. (2011) Cluster Analysis of Glaucoma Patients Using the Retinal Nerve Fiber Layer Thickness of the Optic Nerve and DTI Parameters of the Optic Radiation. J Clinic Experiment Ophthalmol S4:001. doi:10.4172/2155-9570.S4-001

sum of the diffusion in all directions [10,13]. The axial diffusivity (AD) measures the water diffusivity parallel to the axonal fibers [15,16], and the radial diffusivity accounts for water diffusivities perpendicular to the axonal fibers [15,16].

The present study used the cluster analysis to find two different age-groups, who are different in RNFL thickness each independently from glaucoma type. The goal was to investigate the involvement of the optic radiation in glaucoma-induced damage of the optic nerve and to separate this effect from the ageing effect.

Methods

Patients

In the prospective comparative observational study 45 patients clinically diagnosed with glaucoma of different entities (age 60.3±13.0 years) and 17 subjects diagnosed with normal optic nerve head (age 50.3±14.3 years) were randomly selected from the institutional outpatient clinic. Demographic and history data were interrogated by a questionnaire.

Eyes were assessed by ophthalmologic examination including measurement of the retinal nerve fiber layer thickness (RNFL) by Spectralis Optical Coherence Tomography (Heidelberg Engineering, Heidelberg, Germany), automated white-white perimetry (Octo 900 dG2, Interzeag, Schlieren, Switzerland), and measurement of a 24h-profile of the intraocular pressure.

Study participants completed multimodal magnetic resonance imaging of the brain for detection and staging of cerebral microangiopathy and diffusion tensor imaging of the visual pathway for quantification of diffusion and anisotropy parameters within the optic radiation. The MRI readers were blinded to the diagnosis of the study subjects. The study population is characterized in Table 1. None of the subjects had myocardial infarction or carotid endarterectomy.

The study was conducted in accordance with the Declaration of Helsinki on Biomedical Research Involving Human Subjects. The Clinical Investigation Ethics Committee of the University of Erlangen-Nürnberg approved the study protocol, and written informed consent was obtained from all subjects prior to the study after explanation of the nature and possible consequences of the study.

Magnetic resonance imaging

Magnetic resonance imaging was performed on a 3T high-field scanner (Magnetom Tim Trio, Siemens, Erlangen, Germany) with a gradient field strength up to 45 mT/m (72 mT/m effective). The anatomical data were obtained in a T1-weighted 3D-MPRAGE sequence (TR = 900 ms, TE = 3 ms, FoV [field of view] = 23 x 23 cm, acquisition matrix size = 512 x 256 reconstructed to 512 x 512, reconstructed axial plans with 1.2 mm slice thickness). For detection of microangiopathy, a heavily T2-weighted fluid-attenuated inversion recovery (FLAIR) sequence covering the whole brain was acquired (TR = 10,000 ms, TE = 115 ms, matrix size = 512 x 512).

Diffusion tensor imaging

Diffusion tensor imaging was performed in the axial plane with 5 mm slice thickness using a single-shot, spin echo, echo planar imaging (EPI) diffusion tensor sequence covering the whole visual pathway (TR = 3,400 ms, TE = 93 ms, FoV = 23 x 23 cm, acquisition matrix size = 128 x 128 reconstructed to 256 x 256, number of signal averages = 7, partial Fourier acquisition = 60 %). Diffusion weighting with a maximal b-factor of 1,000 s/mm^2 was carried out along 15 icosahedral directions complemented by one scan with b = 0.

Reconstruction of fiber tracts

Datasets were automatically corrected for imaging distorsions and coregistered in reference to T1-weighted MPRAGE images. These and further calculations such as determining the independent elements of the diffusion tensor, deriving the corresponding eigenvalues and eigenvectors, and reconstructing and volume rendering fibers, were performed with a dedicated software package (Neuro 3D, Siemens, Erlangen, Germany).

Algorithm for semi-automated segmentation of the optic radiation

The previously developed algorithm of our group for automated segmentation of the optic radiation in DTI slices is described in detail elsewhere [17]. Briefly, the algorithm relies on the physiological properties of the optic radiation (anterior-posterior diffusion direction) to obtain an automated estimation of the optic radiation. The system uses a statistical surface evolution technique initialized by the estimated optic radiation to segment the optic radiation. Finally, the midbrain is roughly segmented and the segmented optic radiation is refined based on its relative position to the midbrain. The automated segmentation was accomplished in the slice, which soonest included the two lateral geniculate nuclei (LGN) and the largest area of the optic radiation. Then, the estimated segmented optic radiation was checked for concordance with anatomical knowledge and compared to a DTI-based atlases of white matter anatomy [18]. Segmented anatomical structures not belonging to the optic radiation were removed manually. Such structures were the distal part of the optic tract, the forceps major

			Cluster 1 (n=10)	Cluster 2 (n=10)	Cluster 3 (n=19)	Cluster 4 (n=23)
	Male/ female		2/8	5/5	6/13	14/9
Clinical Eye Diagnoses	**Vital Papilla**		10	2	5	0
	Glaucomatous Optic Nerve Atrophy	**NTG**	0	3	5	3
		POAG	0	3	6	14
		SOAG	0	2	3	6
Cardiaovascular risks and events	**Arterial hypertension**		1	1	12	10
	Aorto-coronary bypass surgery		0	0	0	1
	Heart failure, cardiac arrhythmia		0	0	1	3
	Peripheral arterial disease		0	0	0	1

NTG, normal tension glaucoma; **POAG**, primary open angle glaucoma; **SOAG**, secondary open angle glaucoma.
None of the subjects had diabetes, myocardial infarction, stroke, transient ischemic attack, brain tumor, or surgery or stenosis of the carotids.

Table 1: Characteristics of the clusters.

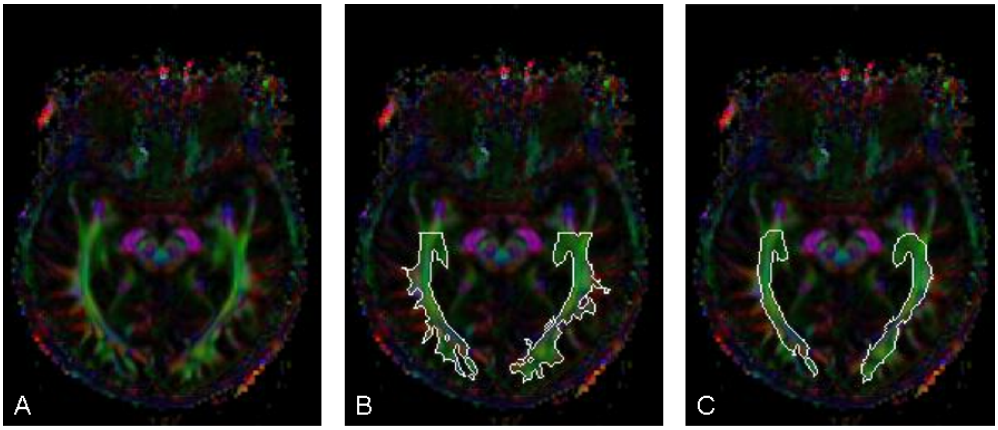

Figure 1. Example of the automated segmentation of the optic radiation and post-processing of the diffusion tensor image. A) Original coloured map of the fractional anisotropy; B) Automated segmentation of the image without correction; C) Manual post-processing.

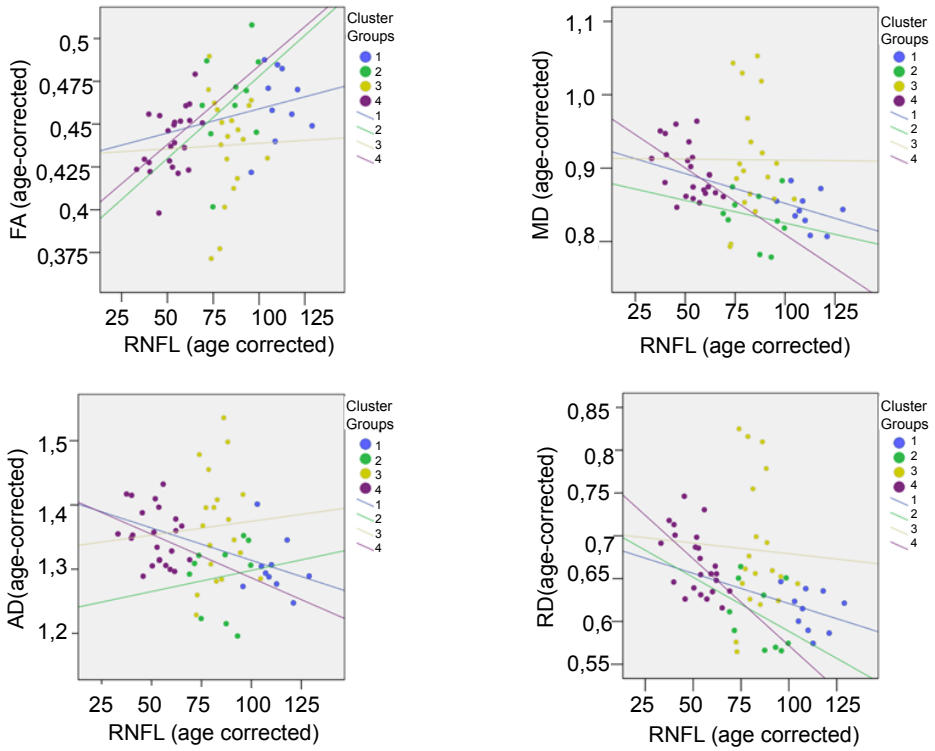

Figure 2. Relationship between DTI variables and RNFL thickness according to cluster groups. The data have been corrected for age. **RNFL**, retinal nerve fiber layer thickness; **FA**, fractional anisotropy; **MD**, mean diffusivity; **AD**, axial diffusivity; **RD**, radial diffusivity.

of the corpus callosum, which proceeds medial of the optic radiations, and all tracts, which do not connect to the primary visual cortex (Figure 1 A-C). The mean of the anisotropy and diffusivity parameters within the segmented areas of the optic radiation was calculated and used for further calculations.

Statistical analysis

Analyses were performed using the PASW software (release 18.0, SPSS Inc. Chicago, IL, USA). Hierarchical cluster analysis was performed to select four groups of patients, two middle-aged and two older groups. The two groups each had different RNFL thickness. The significance of the calculations was confirmed by conventional statistical methods. Normal distribution of the raw data was verified by the Kolmogorov-Smirnov test. Identified groups were compared by means of non-parametric t-test for unpaired samples. For avoidance of a distortion caused by the differently sized measurement values of the DTI-parameters and the RNFL thickness, variables were normalized to z-scores (mean values normalized to 0 and standard deviation normalized to 1) before calculation of the slope. Linear regression analysis was applied to determine the effect of RNFL thickness on the DTI parameters. A p-value ≤ 0.05 was considered to be significant.

Results

The measurement results of the four clusters are shown in Table 2 and 3. Cluster 1 and 2 are characterized by middle age and equal DTI parameters of the optic radiation but different thickness of the retinal nerve fiber layer. Cluster 3 and 4 features an older age and also different RNFL thickness but equal DTI values. The RNFL thickness was not different between the middle-aged group with worse RNFL values and the older group with the better RNFL values within the older groups but the DTI parameters. Cluster 3 and 4 had differently advanced glaucoma as determined by the RNFL values. The slope of the radial diffusivity versus RNFL thickness was different between the two older groups with different RNFL thickness (Table 4). Linear regression analysis showed that in the older patients with the more advanced RNFL reduction (cluster 4) the effect of RNFL reduction was significant on the fractional anisotropy, mean diffusivity, and radial diffusivity of the optic radiations (Table 5).

Discussion

The present study has identified four groups by cluster analysis to investigate the impairment of the optic radiation at different age and with different thickness of the retinal nerve fiber layer. The goal was to identify the variables influencing the condition of the optic radiation.

Comparison of the mean values between groups detected the ageing effect but was not able to prove an additional glaucoma effect in our data. Only the application of regression analysis was able to demonstrate the relationship between clearly reduced RNFL thickness and an impairment of the optic radiation independently from age in advanced glaucoma and anisotropy. This means, that in middle-aged glaucoma patients the diffusivity in the optic radiation appears to be unchanged despite a reduced RNFL thickness. An ascending degeneration from the third to the fourth neuron is not supported by our data in this group. The two older groups consisted predominantly (cluster 3) or exclusively (cluster 4), respectively, of glaucoma patients, but they had a different RNFL thickness, which determines the different progression of optic nerve degeneration. This finding points at an impairment of the axonal integrity/ demyelination of the optic radiation in older glaucoma patients with reduced RNFL thickness, which is independent from ageing effects.

	Total (n=62)	**Cluster 1** (n=10)	**Cluster 2** (n=10)	**Cluster 3** (n=19)	**Cluster 4** (n=23)
Age [years]	57.5±13.8	44.8±9.6	39.6±8.1	67.4±6.4	62.7±9.8
Fractional Anisotropy	0.447±0.027	0.462±0.021	0.464±0.029	0.438±0.031	0.440±0.018
Mean Diffusivity [10^{-3} mm^2 s^{-1}]	0.882±0.063	0.843±0.028	0.834±0.035	0.911±0.086	0.896±0.039
Axial Diffusivity [10^{-3} mm^2 s^{-1}]	1.338±0.071	1.303±0.047	1.288±0.056	1.367±0.092	1.351±0.047
Radial Diffusivity [10^{-3} mm^2 s^{-1}]	0.654±0.063	0.613±0.027	0.607±0.039	0.683±0.085	0.669±0.039
Mean Retinal Nerve Fiber Layer [µm]	75.7±23.0	111.0±9.7	79.1±11.0	83.7±9.9	52.3±9.7
Retinal Nerve Fiber Layer OD [µm]	77.4±25.0	110.9±9.9	84.4±10.9	87.5±10.5	51.5±15.3
Retinal Nerve Fiber Layer OS [µm]	74.9±25.0	111.3±10.0	73.6±17.6	79.9±15.0	55.4±19.1
Mean Deviation of OD [dB]	5.9±7.5	-0.3±1.1	2.2±5.1	2.0±3.3	12.7±7.1
Mean Deviation of OS [dB]	6.4±8.5	0.3±1.9	3.4±8.9	2.9±3.8	13.4±8.7
Best Corrected Visual Acuity OD [decimal]	0.8±0.3	1.0±0.1	0.9±0.2	0.8±0.3	0.7±0.3
Best Corrected Visual Acuity OS [decimal]	0.7±0.3	0.9±0.3	0.8±0.3	0.8±0.2	0.6±0.3
Treated Tensio OD [mmHg]	15.2±4.5	14.9±3.2	14.9±2.0	14.2±3.5	16.3±6.3
Treated Tensio OS [mmHg]	15.8±5.9	15.1±2.6	17.9±9.8	14.1±3.1	16.6±6.5

OD, right eye; **OS**, left eye; **FA**, fractional anisotropy; **MD**, mean diffusivity; **AD**, axial diffusivity, **RD**, radial diffusivity; **RNFL**, retinal nerve fiber layer thickness.

Table 2: Measurements and age classified into clusters. The mean ± SD are given.

	Cluster Group					
	1 vs. 2	**3 vs. 4**	**1 vs. 3**	**1 vs. 4**	**2 vs. 3**	**2 vs. 4**
Age [years]	0.306	0.168	<0.001	<0.001	<0.001	<0.001
Fractional Anisotropy	0.762	0.695	0.028	0.008	0.039	0.011
Mean Diffusivity [10^{-3} mm^2 s^{-1}]	0.734	0.850	0.007	0.001	0.005	0.001
Axial Diffusivity [10^{-3} mm^2 s^{-1}]	0.880	0.919	0.020	0.006	0.046	0.012
Radial Diffusivity [10^{-3} mm^2 s^{-1}]	0.734	0.879	0.007	<0.001	0.004	0.002
Mean RNFL [µm]	<0.001	<0.001	<0.001	<0.001	0.313	<0.001
RNFL OD [µm]	<0.001	<0.001	<0.001	<0.001	0.535	<0.001
RNFL OS [µm]	<0.001	<0.001	<0.001	<0.001	0.347	0.014
Mean Deviation of OD [dB]	0.248	<0.001	0.126	<0.001	0.886	<0.001
Mean Deviation of OS [dB]	0.350	<0.001	0.113	<0.001	0.614	0.006
VA of OD [decimal]	0.744	0.097	0.164	0.003	0.247	0.018
VA of OS [decimal]	0.417	0.309	0.120	0.040	0.565	0.199
Tensio OD [mmHg]	0.849	0.381	0.562	0.738	0.404	0.829
Tensio OS [mmHg]	0.376	0.501	0.418	0.890	0.249	0.582

OD, right eye; **OS**, left eye; **FA**, fractional anisotropy; **MD**, mean diffusivity; **AD**, axial diffusivity, **RD**, radial diffusivity; **RNFL**, retinal nerve fiber layer thickness; **VA**, best corrected visual acuity.

Table 3: Comparison between clusters. The p-values of the non-parametric t-test for unpaired samples are given.

		Cluster 1	Cluster 2	Cluster 3	Cluster 4	Cluster groups		
						1 vs. 2	3 vs. 4	2 vs. 3
Corrected for age	RNFL	111.03±9.58	85.06±11.85	83.71±8.58	52.28±9.55	<0.001	<0.001	0.783
	FA	0.46±0.02	0.46±0.03	0.44±0.03	0.44±0.02	0.762	0.752	0.028
	MD	0.84±0.02	0.83±0.04	0.91±0.08	0.90±0.04	0.597	0.870	0.003
	AD	1.30±0.04	1.29±0.06	1.37±0.08	1.35±0.04	0.821	0.714	0.022
	RD	0.61±0.02	0.61±0.04	0.68±0.08	0.67±0.04	0.650	0.850	0.009
Corrected for age and normalized to Z score	FA/ RNFL	0.36±0.70	2.21±7.19	-1.88±11.06	0.11±0.81	0.226	0.056	0.035
	MD/ RNFL	-0.45±0.26	0.50±3.12	3.00±10.00	-0.12±0.60	1.000	0.120	0.271
	AD/ RNFL	-0.37±0.52	1.99±7.18	2.96±10.93	-0.13±0.70	0.199	0.185	0.680
	RD/ RNFL	-0.46±0.26	-0.38±2.37	2.84±10.07	-0.11±0.63	0.450	0.025	0.039

FA, fractional anisotropy; **MD**, mean diffusivity; **AD**, axial diffusivity, **RD**, radial diffusivity; **RNFL**, retinal nerve fiber layer thickness.

Table 4: Differences of DTI variables and RNFL thickness between cluster groups. The mean ± SD and p-values are given.

	Cluster Group	Regression Coefficient (unstandardized)	Std. Error	Regression Coefficient (standardized)	*P*	95.0% Confidence Interval
FA	1	0.0003	0.0008	0.128	0.725	-0.0015 to 0.0021
	2	0.0010	0.0008	0.389	0.266	-0.0009 to 0.0028
	3	0.0001	0.0009	0.018	0.940	-0.0018 to 0.0019
	4	0.0009	0.0004	0.485	0.019	0.0002 to 0.0017
MD	1	-0.0008	0.0009	-0.314	0.377	-0.0028 to 0.0012
	2	-0.0006	0.0010	-0.208	0.564	-0.0030 to 0.0017
	3	0.0000	0.0022	-0.003	0.991	-0.0047 to 0.0047
	4	-0.0018	0.0007	-0.477	0.021	-0.0033 to -0.0003
AD	1	-0.0010	0.0015	-0.225	0.533	-0.0046 to 0.0026
	2	0.0007	0.0017	0.139	0.703	-0.0032 to 0.0045
	3	0.0004	0.0024	0.044	0.859	-0.0046 to 0.0055
	4	-0.0014	0.0009	-0.298	0.167	-0.0033 to 0.0006
RD	1	-0.0007	0.0009	-0.277	0.438	-0.0027 to 0.0013
	2	-0.0013	0.0011	-0.383	0.275	-0.0037 to 0.0012
	3	-0.0002	0.0022	-0.027	0.912	-0.0049 to 0.0044
	4	-0.0020	0.0007	-0.527	0.010	-0.0035 to -0.0005

FA, fractional anisotropy; **MD**, mean diffusivity; **AD**, axial diffusivity, **RD**, radial diffusivity; **RNFL**, retinal nerve fiber layer thickness.

Table 5: Effect of age-corrected RNFL thickness on age-corrected DTI Parameters by linear regression analysis.

In general, the fractional anisotropy (FA) and mean diffusivity (MD) have been described to denote the axonal integrity of neuronal tracts [10,13,14], whereas the radial diffusivity (RD) increases with the degree of demyelination or glial cell morphology [15]. MD and FA are known to be sensitive to white matter pathologies, but with lacking specificity of the differentiation between different pathologies (e.g. acute stroke, multiple sclerosis, cerebral tumors). Thus, the explanatory power of these measures is limited [20-22].

The increase of the mean diffusivity in the optic radiation was also observed with ageing and is thought to agree with the pattern of a chronic ischemic process independent from other risk factors and diseases [23]. Ageing is associated with an increase of the radial diffusivity. There is close agreement between neuropathology and imaging measures suggesting that ageing underlies the process of myelin breakdown [24].

The impact of ischemic processes on the visual pathway has been examined by *in vivo* DTI in a mouse model of optic nerve degeneration resulting from transient retinal ischemia [25]. The death of retinal ganglion cells caused an early and prolonged decrease of diffusion anisotropy (FA) in the optic nerve. A pattern of gradual MD increase after a sharp early decrease of MD in the optic nerve was seen also in stroke [10]. During transient ischemia AD and RD have shown distinct patterns with an early and prolonged decrease of AD and a delayed and sustained elevation of RD [25-27]. Ostensible normalization of MD during follow-up was interpreted as a result of combined axonal injury and demyelination [10]. This pattern reflects the histological profile of axonal injury preceding myelin injury without significant destruction of overall axonal cytoskeletons [25-27]. However, these findings are attributed to acute impairment of the visual pathway within a few weeks. In chronic optic nerve atrophy another pattern of DTI parameter changes could be the result of damage through several years.

An association between defects of the retinal nerve fiber layer and signs of cerebral ischemia has been described particularly in older male subjects, who suffer from arterial hypertension [28]. Indeed, the older clusters in our study had a high prevalence of arterial hypertension and also the retinal nerve fiber layer thickness was reduced compared to the middle-aged clusters.

In conclusion, in middle-aged glaucoma patients degeneration of the optic radiation may not be detected by the methods applied in this study. In older glaucoma patients damage of the axonal integrity and demyelination of the optic radiation is suggested to be predominantly induced by ageing, which may cover the additional effect by advanced glaucomatous RNFL impairment.

Acknowledgement

This study was supported by the Federal Ministry of Education and Research (BMBF), Bonn, Germany (excellence cluster Medical Valley EMN, Grant MVEMN-A-02).

The authors declare that they had full access to all the data in the study and had final responsibility for the decision to submit for publication. All authors declare that they have no conflict of interest.

G. Michelson and S. Wärntges contributed equally to this work and thus, share first authorship.

References

1. Burr JM, Mowatt G, Hernández R, Siddiqui MAR, Cook J, et al. (2007) The clinical effectiveness and cost-effectiveness of screening for open angle glaucoma: a systematic review and economic evaluation. Health Technol Assess 11: 1-190.
2. Yücel YH, Zhang Q, Weinreb RN, Kaufman PL, Gupta N (2003) Effects of retinal ganglion cell loss on magno-, parvo-, koniocellular pathways in the lateral geniculate nucleus and visual cortex in glaucoma. Prog Retin Eye Res 22: 465-481.
3. Weber AJ, Chen H, Hubbard WC, Kaufman PL (2000) Experimental glaucoma and cell size, density, and number in the primate lateral geniculate nucleus. Invest Ophthalmol Vis Sci 41: 1370-1379.
4. Gupta N, Ang LC, Noël de Tilly L, Bidaisee L, Yücel YH (2006) Human glaucoma and neural degeneration in intracranial optic nerve, lateral geniculate nucleus, and visual cortex. Br J Ophthalmol 90: 674-678.
5. van Swieten JC, Geyskes GG, Derix MM, Peeck BM, Ramos LM, et al. (1991) Hypertension in the elderly is associated with white matter lesions and cognitive decline. Ann Neurol 30: 825-830.
6. Liao D, Cooper L, Cai J, Toole J, Bryan N (1997) The prevalence and severity of white matter lesions, their relationship with age, ethnicity, gender, and cardiovascular disease risk factors: the ARIC Study. Neuroepidemiology 16: 149-162.
7. Wen W, Sachdev PS (2004) Extent and distribution of white matter hyperintensities in stroke patients: the Sydney Stroke Study. Stroke 35: 2813-2819.
8. Breteler MM, van Swieten JC, Bots ML, Grobbee DE, Claus JJ, et al. (1994) Cerebral white matter lesions, vascular risk factors, and cognitive function in a population-based study: the Rotterdam Study. Neurology 44: 1246-1252.
9. Pierpaoli C, Jezzard P, Basser PJ, Barnett A, DiChiro G (1996) Diffusion tensor MR imaging of the human brain. Radiology 201: 637-648.
10. Sotak CH (2002) The role of diffusion tensor imaging in the evaluation of ischemic brain injury - a review. NMR Biomed.;15: 561-569.
11. Le Bihan D, Breton E, Lallemand D, Grenier P, Cabanis E, et al. (1986). MR imaging of intravoxel incoherent motions: application to diffusion and perfusion in neurologic disorders. Radiology 161: 401–407.
12. Basser PJ, Pierpaoli C (1996) Microstructural and physiological features of tissues elucidated by quantitative-diffusion-tensor MRI. J Magn Reson B 111: 209–219.
13. Xu J, Sun SW, Naismith RT, Snyder AZ, Cross AH, et al. (2008) Assessing optic nerve pathology with diffusion MRI: from mouse to human. NMR Biomed 2: 928-940.
14. Dong Q, Welsh RC, Chenevert TL, Carlos RC, Maly-Sundgren P, et al. (2004) Clinical applications of diffusion tensor imaging. J Magn Reson Imaging 19: 6-18.
15. Song SK, Sun SW, Ju WK, Lin SJ, Cross AH, et al. (2003) Diffusion tensor imaging detects and differentiates axon and myelin degeneration in mouse optic nerve after retinal ischemia. Neuroimage 20: 1714–1722.
16. Song SK, Sun SW, Ramsbottom MJ, Chang C, Russell J, et al. (2002) Dysmyelination revealed through MRI as increased radial but unchanged axial diffusion of water. Neuroimage 17: 1429–1436.
17. El-Rafei A, Hornegger J, Engelhorn T, Dörfler A, Wärntges S, et al. (2009) Automatic Segmentation of the Optic Radiation using DTI in Glaucoma Patients. In: Tavares, João Manuel RS, Jorge RM Natal (eds.): Computational Vision and Medical Image Processing – VipIMAGE (International Conference VipIMAGE 2009 – II ECCOMAS THEMATIC CONFERENCE ON COMPUTATIONAL VISION AND MEDICAL IMAGE PROCESSING, Porto, Portugal, 14-16.10.2009). Portugal: Taylor and Francis: 293-298.
18. Wakana S, Jiang H, Nagae-Poetscher LM, van Zijl PC, Mori S (2004) Fiber tract-based atlas of human white matter anatomy. Radiology 230: 77-87.
19. Kaufman L, Rousseeuw P (1990) Finding Groups in Data: An Introduction to Cluster Analysis. New York: Wiley
20. Mukherjee P (2005) Diffusion tensor imaging and fiber tractography in acute stroke. Neuroimaging Clin N Am 15: 655–665.
21. Ge Y, Law M, Grossman RI (2005) Applications of diffusion tensor MR imaging in multiple sclerosis. Ann N Y Acad Sci 1064: 202–219.
22. Field AS, Alexander AL (2004) Diffusion tensor imaging in cerebral tumor diagnosis and therapy. Top Magn Reson Imaging 15: 315–324.
23. Fazekas F, Schmidt R, Scheltens P. Pathophysiologic mechanisms in the development of age-related white matter changes of the brain. Dement Geriatr Cogn Disord 1: 2-5.
24. Bartzokis G, Lu PH, Mintz J (2004) Quantifying age-related myelin breakdown with MRI: novel therapeutic targets for preventing cognitive decline and Alzheimer's disease. J Alzheimers Dis 6: S53-59.
25. Sun S-W, Liang H-F, Cross AH, Song SK (2008) Evolving Wallerian degeneration after transient retinal ischemia in mice characterized by diffusion tensor imaging. Neuroimage 40: 1-10.
26. Song SK, Sun SW, Ju WK, Lin SJ, Cross AH, et al. (2003) Diffusion tensor imaging detects and differentiates axon and myelin degeneration in mouse optic nerve after retinal ischemia. Neuroimage.; 20: 1714–1722.
27. Sun SW, Liang HF, Le TQ, Armstrong RC, Cross AH, et al. (2006) Differential sensitivity of in vivo and ex vivo diffusion tensor imaging to evolving optic nerve injury in mice with retinal ischemia. Neuroimage 32: 1195–1204.
28. Yüksel N, Anik Y, Altintaş O, Onur I, Cağlar Y, et al. (2006) Magnetic resonance imaging of the brain in patients with pseudoexfoliation syndrome and glaucoma. Ophthalmologica 220: 125-130.

This article was originally published in a special issue, **Glaucoma** handled by Editor(s). Dr. Zaher Sbeity, University of Dusseldorf Teaching Hospital, Germany